



ELSEVIER

Ecological Modelling 90 (1996) 53–67

ECOLOGICAL
MODELLING

Comparison of alternative spatial resolutions in the application of a spatially distributed biogeochemical model over complex terrain¹

David P. Turner^{a,*}, Rusty Dodson^a, Danny Marks^b

^a ManTech Environmental Research Services Corporation, U.S. EPA Environmental Research Laboratory, 200 S.W. 35th Street, Corvallis, OR 97333, USA

^b U.S. Geological Survey, U.S. EPA Environmental Research Laboratory, 200 S.W. 35th Street, Corvallis, OR 97333, USA

Received 22 November 1994; accepted 23 June 1995

Abstract

Spatially distributed biogeochemical models may be applied over grids at a range of spatial resolutions, however, evaluation of potential errors and loss of information at relatively coarse resolutions is rare. In this study, a georeferenced database at the 1-km spatial resolution was developed to initialize and drive a process-based model (Forest-BGC) of water and carbon balance over a gridded 54976 km² area covering two river basins in mountainous western Oregon. Corresponding data sets were also prepared at 10-km and 50-km spatial resolutions using commonly employed aggregation schemes. Estimates were made at each grid cell for climate variables including daily solar radiation, air temperature, humidity, and precipitation. The topographic structure, water holding capacity, vegetation type and leaf area index were likewise estimated for initial conditions. The daily time series for the climatic drivers was developed from interpolations of meteorological station data for the water year 1990 (1 October 1989–30 September 1990). Model outputs at the 1-km resolution showed good agreement with observed patterns in runoff and productivity. The ranges for model inputs at the 10-km and 50-km resolutions tended to contract because of the smoothed topography. Estimates for mean evapotranspiration and runoff were relatively insensitive to changing the spatial resolution of the grid whereas estimates of mean annual net primary production varied by 11%. The designation of a vegetation type and leaf area at the 50-km resolution often subsumed significant heterogeneity in vegetation, and this factor accounted for much of the difference in the mean values for the carbon flux variables. Although area-wide means for model outputs were generally similar across resolutions, difference maps often revealed large areas of disagreement. Relatively high spatial resolution analyses of biogeochemical cycling are desirable from several perspectives and may be particularly important in the study of the potential impacts of climate change.

Keywords: Biogeochemistry; Climate; Production, primary; Scale; Spatial patterns; Water dynamics

* Corresponding author. E-mail: dave@mail.cor.epa.gov; Fax: (+1-503) 754-4818.

¹ The research described in this manuscript has been funded in part by the U.S. Environmental Protection Agency. This manuscript has been prepared at the EPA Environmental Research Laboratory in Corvallis, Oregon, through contract number 68-C4-0019 to ManTech Environmental Research Services Corporation. It has been subjected to the Agency's peer and administrative review and approved for publication. Mention of trade names or commercial products does not constitute endorsement or recommendation for use.

1. Introduction

Spatially-distributed biogeochemistry models are needed for understanding current spatial and temporal patterns in runoff and plant productivity, as well as evaluating potential ecological effects of climate change and land use change. Band et al. (1991) have identified the potential bias in distributed modeling which is introduced by employing landscape mean values for input variables when using a model with significant nonlinear responses to those driving variables. This consideration, as well as others related to factors including the scale of relevant disturbances, the benefits of examining vegetation characteristics along environmental gradients, and the interest in localized responses to factors such as climate change, support the general goal of retaining high spatial resolution in these modeling efforts. However, as the spatial resolution is increased for a given area, or a high spatial resolution is retained as the domain of interest is enlarged, computational speed and on-line data storage become increasing constraints.

The availability of high-resolution digital elevation data has recently made it feasible to simulate climatic drivers such as temperature and radiation at high spatial resolution. The availability of satellite imagery has likewise promoted the development of high spatial resolution land cover maps (Loveland et al., 1991) and surfaces for features such as leaf area index (Running et al., 1989). These advances provide the opportunity to evaluate the effects of using highly resolved as opposed to highly aggregated inputs for a spatially distributed biogeochemistry model.

In this study, a database was developed to run the Forest-BGC model (Running and Coughlan, 1988) over a 1-km grid covering a 54976-km² region in western Oregon. Simulation results for annual water and carbon flux variables at the 1-km spatial resolution were compared with those using climatic and land surface inputs at coarser spatial resolutions. The 1-km resolution was used as the finest spatial resolution because of the availability of land cover maps based on the satellite-borne Advanced Very High Resolution Radiometer (AVHRR) sensor which has an approximate spatial resolution of 1-km (Loveland et al., 1991). The study area is representative of the topography encountered over much of the mountain-

ous western U.S. The specific objective was to examine the degree of similarity between outputs from simulations run over grids at the 1-, 10-, and 50-km resolutions covering this heterogeneous region.

2. Methods

The spatial domain (extent) in the study covered two adjacent river basins, the Willamette (28960 km²) and the Deschutes (26725 km²) in western Oregon (Fig. 1a, b, c). The Cascade Mountain Range divides the study area and elevation ranges from 6 to 3084 m. Vegetation cover includes cropland, shrubland, forest and alpine tundra (Franklin and Dyrness, 1990).

Digital maps of the land-surface characteristics needed to initialize the model, and digital maps of the climatic drivers needed to drive the model, were initially developed at the 1-km resolution (grid cells 1 km on a side). A somewhat larger area than the two river basins was used in order to avoid artifacts associated with abrupt edges. The climate surfaces were based on interpolations of time series data (water year 1990) from a network of meteorological stations. In order to run the model at coarser resolutions (10 or 50 km), a new set of land surface and climatic drivers were assembled using a coarse-resolution Digital Elevation Model (DEM). Comparison among inputs prepared at the different spatial resolutions, and outputs for the simulations run at different spatial resolutions, were made based on averages, ranges, and difference maps over the entire area.

2.1. The model

Forest-BGC is a stand level model which has been applied over spatial grids at the watershed to regional scale for analysis of the carbon, nitrogen and water cycles (Running and Coughlan, 1988; Band et al., 1991; Running and Gower, 1991). A few simple compartments – including foliage, stems and roots – are used rather than representations of individual trees. The focus is on incorporating basic plant physiology and biophysics in a very general fashion in order to simulate effects of climatic gradients or climatic change on ecosystem mass flux. Processes including photosynthesis, maintenance res-

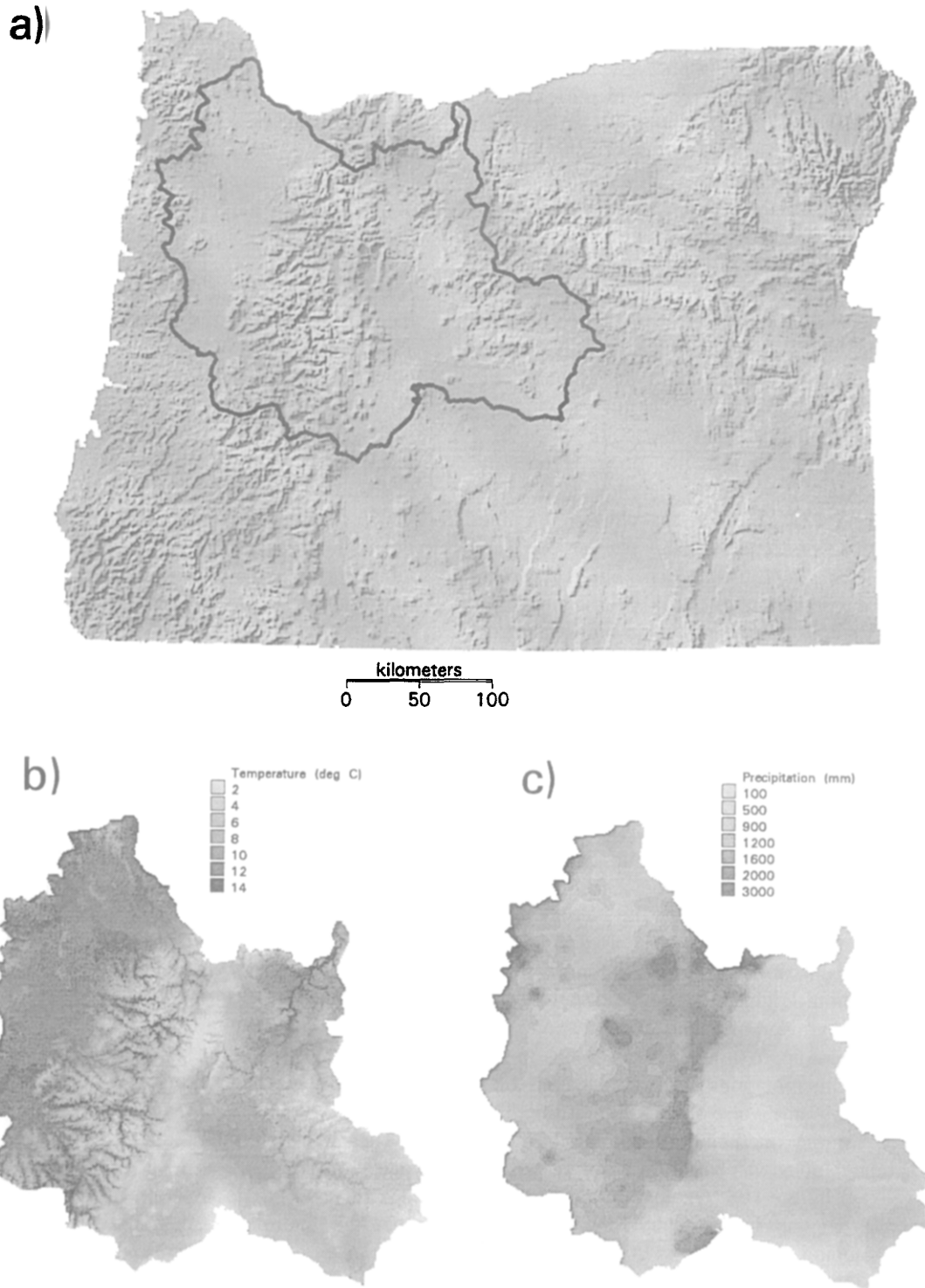


Fig. 1. (a) Shaded relief map of Oregon indicating the study area. (b) Mean annual temperature over the study area. (c) Annual precipitation over the study area.

piration, evaporation, and transpiration are simulated at a daily time step whereas allocation of assimilated carbon among the plant parts and decomposition are simulated annually. Species are not identified, however, the model may be run in three modes based on life form (conifer, broadleaf or grass), with physiological variables such as maximum stomatal conductance varying by life form (Running and Hunt, 1993). Comparison of model outputs, such as aboveground net primary production and site water balance, to observed patterns of carbon and water flux have indicated reasonable agreement for a range of environments (Running and Coughlan, 1988; Running and Nemani, 1988; Hunt et al., 1991; Running and Hunt, 1993).

To adapt the model from the point mode to a spatially distributed mode, the Image Processing Workbench (Frew, 1990) was employed such that multiple band (image) files for climate variables (i.e., one image or surface per day per variable), and spatially varying land surface characteristics, were available for assembly of grid-cell-specific input files. The model could then be run point-by-point across the grid of interest with retention of user-defined daily or annual outputs as images.

2.2. Data inputs

2.2.1. Climatic variables

The daily climatic variables needed to drive Forest-BGC are minimum and maximum temperature, dew point temperature, precipitation, and solar radiation. Daily time series data from the National Climate Data Center and Snotel meteorological station networks (described in Earth Info, 1988 and USDA, Soil Conservation Service, 1988) provided the basis for distributed temperature and precipitation surfaces. There were approximately 100 stations in the study area and interpolations of the climate variables were made using an inverse squared algorithm. The DEM used for the interpolations and in the solar radiation calculations was based on a 15-arc-second grid developed by the U.S. Geological Survey from 3-arc-second Digital Topographic Elevation Data (Defense Mapping Agency, 1981). The DEM was re-projected into an Albers Equal Area projection at 1-km using a bi-linear interpolation algorithm (Fig. 1).

For temperatures, daily meteorological station data for maximum and minimum temperature values were first converted to their sea level equivalents using the assumption of locally adiabatic conditions (Kimball, 1992). An interpolation was then made over the grid and all values were adjusted to their elevation in the DEM by inverting the conversion procedure. The dew-point temperature was assumed to be the minimum daily temperature (Running et al., 1987; Glassy and Running, 1994). The precipitation surfaces were prepared initially at the 10-km resolution from monthly outputs of the PRISM model (Daly et al., 1994). PRISM is a moving window regression model which requires monthly precipitation from a network of meteorological stations and a DEM as inputs. For each grid cell, the model determines a geomorphic facet (such as a portion of the west side of the Cascade Mountains) for which there are sufficient meteorological stations to construct a regression of precipitation against elevation. For the daily precipitation surfaces, the proportion of the monthly precipitation observed on a given day at each station was used to create daily proportionality surfaces and these were applied to the monthly precipitation surfaces which had also been interpolated to the 1-km resolution.

Clear sky short wave solar irradiance (0.3–1.1 μm) was calculated using the topographically corrected spectral radiation model described by Dubayah et al. (1990), and modified for regional application by Marks et al. (1991). The principal model inputs are elevation and surface albedo, with albedo obtained from AVHRR imagery (USGS, 1991). The adjustment for cloud cover effects was based on differences between daily minimum and maximum temperature (Bristow and Campbell, 1984; Glassy and Running, 1994).

2.2.2. Site variables

The site variables required by Forest-BGC include vegetation type, leaf area index, soil water holding capacity, and biomass carbon pools. For vegetation type, the multiple vegetation classes in the land cover map (1-km spatial resolution) of Loveland et al. (1991), which is based on the temporal Normalized Difference Vegetation Index (NDVI) signal from the AVHRR sensor, were aggregated to three

biome-level classes designated as conifer, shrubland, and grassland.

land et al. (1991) with estimates from a ground-based forest inventory (Waddell et al., 1989) revealed close correspondence in Oregon (Turner et al., 1993).

Comparison of forest cover estimates from Love-

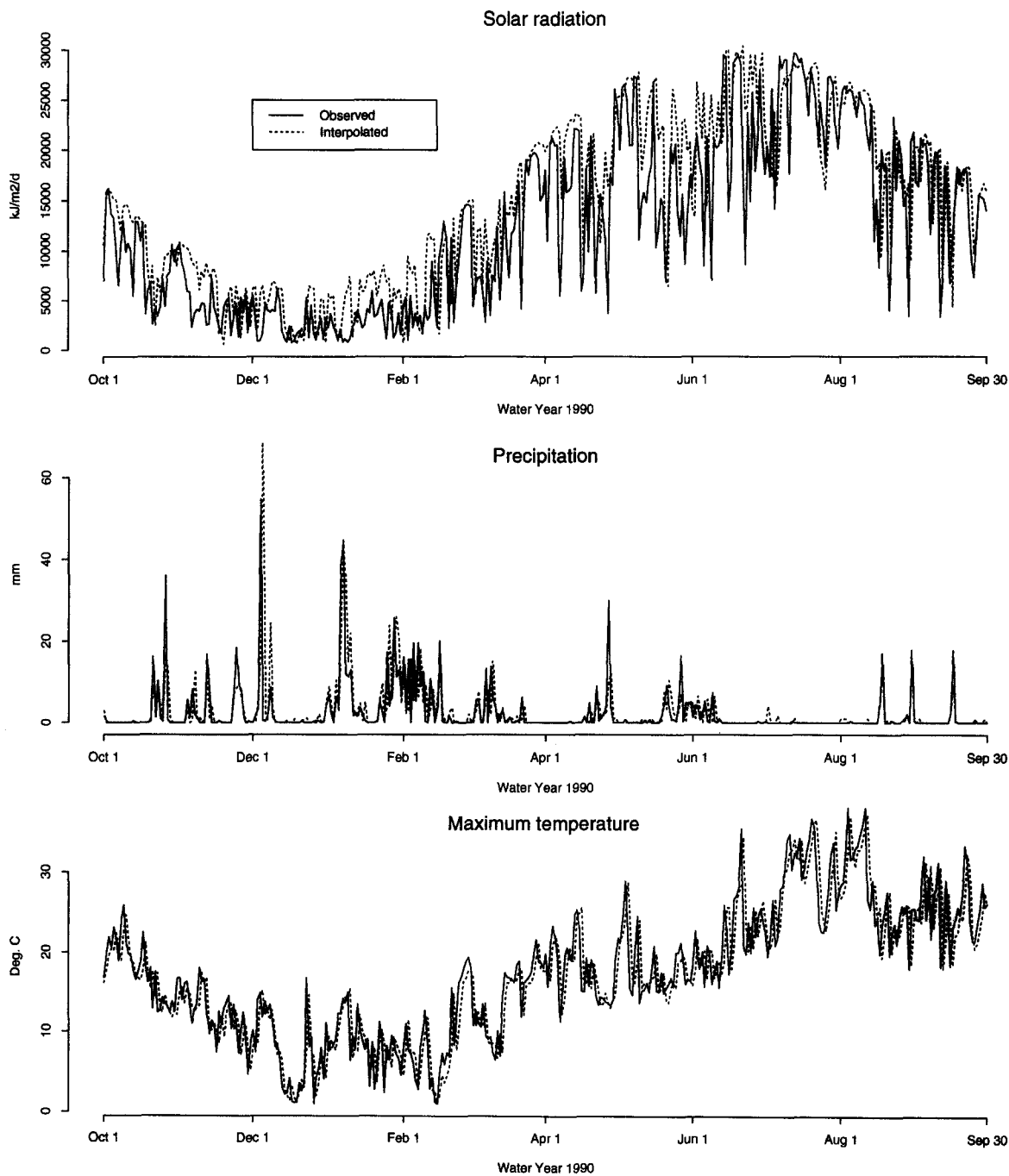


Fig. 2. Comparison of observed and interpolated values for temperature, radiation, and precipitation (water year 1990) near Corvallis, Oregon. The nearest meteorological station used in the interpolation was 6 km away. Values are offset one day to facilitate comparison.

Output from Forest-BGC is strongly influenced by LAI. Field studies at the Thematic Mapper resolution (~ 30 m; Peterson et al., 1987) and the AVHRR resolution (~ 1 km; Running et al., 1989) have indicated promise for developing remote-sensing-based algorithms which could be used for initializing LAI over forested regions. However, the relationship of indices such as NDVI to LAI tends to be asymptotic, and LAIs in cool coniferous forests of the Pacific Northwest may be towards the high end of the potential LAI range, thus the sensitivity of LAI to NDVI may be low in parts of this region.

An alternative approach relies on developing a regression of an index of site water balance against observed LAIs. Much current theory on the relationship of climate to vegetation type and LAI holds that site LAI will rise to a level which uses as much available water as possible without leaving the water supply depleted over an extended period (Woodward, 1987; Nemani and Running, 1989; Neilson et al., 1992). Therefore an index of annual or growing season site water balance should correlate with LAI and provide the basis for preparing an LAI surface. Grier and Running (1977) found evidence for such a relationship in the coniferous forests of the Pacific Northwest.

In order to generate a potential LAI for the forested grid cells in this study area, a water balance index (WBI) was calculated over the region and used to develop an algorithm relating WBI and observed LAIs. A WBI surface (10-km spatial resolution) was constructed by subtracting the May–September sum of potential evapotranspiration (PET) from the May–September sum of precipitation. Long-term average monthly precipitation surfaces were derived from meteorological station data interpolated using the PRISM model (C. Daly, Oregon State University, pers. commun.) and monthly PET surfaces were from Dolph et al. (1992). Measured LAIs (projected) based on an allometric approach, with approximate locations, were from Peterson et al. (1987). Six of the seven sites used in the regression were located in the study area and the sites included stands in the Juniper (*Juniperus occidentalis*) woodland of eastern Oregon and conifer stands at a range of elevations in the Cascade Mountains.

The relationship between measured LAI and the corresponding WBI was nearly linear (seven sites,

$R^2 = 0.67$, $P = 0.02$) as was the similar relationship found by Grier and Running (1977). After using the WBI surface to generate an LAI surface at the 10-km resolution, an interpolation to 1-km was made using the inverse distance squared weighting algorithm and the nearest four neighbors. Finally, an LAI limit of 8 was imposed on the LAI surface because of uncertainties about the high LAIs reported for the Pacific Northwest coniferous forests using the allometric approach (Marshall and Waring, 1986). LAI was fixed at 1 for shrubland grid cells and 2 for grassland grid cells based on regional averages for foliar biomass production in those vegetation types (King, 1993).

The soil water holding capacity was calculated as the difference in water content at a matric potential of -33 kPa and at -1500 kPa. Estimates for these water contents (Kern, 1995) were based on particle size distribution data using algorithms from Saxton et al. (1986). Water holding capacity was adjusted for the amount of soil present by accounting for rock fragment content and depth to bedrock. The particle size distribution, rock fragment content, and depth to bedrock were estimated using the USDA Soil Conservation Service's state soil geographic database (STATSGO) that was compiled at a map scale of 1:250 000 (Soil Conservation Service, 1991). The smallest polygons on the base WHC map were on the order of several km across, suggesting a somewhat coarser resolution than is indicated by the 1-km sampling of the base map.

Foliar carbon was calculated from the estimated LAI and the specific leaf area conversion factors in Running and Hunt (1993). The assumption was made that all forest stands were 50 years of age with a stem biomass of 50 000 kg/ha, thus, the results are an indication of potential net primary productivity. Because of the large uncertainties about foliar nitrogen concentrations and nitrogen mineralization rates in soil and litter, the nitrogen cycle component of Forest-BGC was not included in this analysis.

2.3. Ten- and 50-km resolutions

The issue of how best to aggregate fine-scale data to a coarser resolution is complex, and the optimal approach is to some degree unique to each variable. For this analysis, the general approach was to take

the fine-scale value at the center point of each coarse-resolution grid cell as the representative value for the coarse-resolution cell. Alternative algorithms, such as taking the average or mode of the 1-km cells within each coarse-resolution cell, were considered but the center-point approach was chosen because it retains the possibility of maintaining the complete distribution of the values at the finer resolution.

New temperature surfaces were created at 10- and 50-km resolutions using the same set of meteorological stations and procedures but the center-point-sampled DEMs. The radiation surfaces were also recreated and were impacted by the coarser DEMs via differences in elevation, slope, and aspect. Precipitation was originally generated at the 10-km resolution (Daly et al., 1994) and for the 50-km simulation, the center-point sampling algorithm was again used.

The land surface characteristics include both categorical and continuous variables. Biome type is a categorical variable and the modal type among the 1-km cells within each 10- or 50-km cell became the representative type. If the modal biome type was grassland or shrubland, the biome-specific LAI was assigned. If the modal biome type was forest, the LAI was taken from the base 10-km LAI map. In the case of the 50-km simulation, the average LAI for all 1-km cells classified as forest was calculated from the base 10-km LAI map and used for a representative value. Foliar and stem carbon were estimated as in the 1-km simulation. Soil water holding capacity was generated by sampling the center points of the coarse-resolution grid cells.

For comparison of outputs at the different resolutions, the 1-km resolution outline (mask) of the river basins was overlaid on the coarse-resolution outputs. Ranges and area weighted means were then calculated using IPW.

3. Results

The DEM (Fig. 1a) reveals the general topographic features of the region. These include the broad Willamette Valley in the west, the north–south running Cascade Range in the center and the high plateau region of the Deschutes River Basin in the east. Conifer forests dominate the Cascade Range, with shrubland to the east and grassland in the

Willamette Valley. Estimated LAIs were highest at mid-elevations in the mountainous regions where relatively high precipitation and mild temperature generate a strongly positive growing season water balance (Fig. 1b, c).

3.1. One-km simulation

The daily minimum and maximum temperature surfaces had the expected elevational gradients and seasonal trends. Clear sky radiation surfaces revealed mountain tops and topographic effects such as north- and south-facing slopes. Annual precipitation displayed the east–west gradient characteristic of this region, with highest values along the crest of the Cascade Mountains (Fig. 1c). Comparisons of interpolated temperature, radiation and precipitation values with independent daily observations at several sites generally showed good agreement (e.g., Fig. 2).

Because of the relatively low summer precipitation in the Pacific Northwest, the annual time course of soil moisture typically displays a late summer trough with recharge in the fall (Running, 1994). Point-mode model runs at a variety of sites around the study area also showed this pattern. Declines in soil water availability induce reductions in leaf water potential and this relationship offers some opportunity for checks on simulated water balance at the site level. Seasonal measurements of leaf water potential were made in association with the Oregon Transect for Ecosystem Research (OTTER) in the summer of 1990 for five sites within the study region (Runyon et al., 1994). Comparison of the magnitude and timing of water stress between those observations and the model output at the same points generally yielded good agreement. Running (1994) discusses possible reasons for a difference between observed and modeled water stress at one of the sites where contributions to the water budget from upslope or lateral flow may have been significant.

Comparisons of modeled water balance with observations were also made at the river basin scale. Water year runoff for 1990 at the mouth of the Willamette River was 83 cm averaged over the basin (Hubbard et al., 1991). The simulated average runoff in the simulation was 80 cm over the same area. Evaporation plus transpiration accounted for 39% of precipitation with 60% of total evapotranspiration as

Table 1
Comparison of mean and range for climate inputs (1 June) across spatial resolutions

Resolution (km)	Clear sky radiation (kJ/m ² /d)			T min (°C)			T max (°C)		
	Mean	Min	Max	Mean	Min	Max	Mean	Min	Max
1	22 039	7141	24 792	1.4	-17.7	9.5	12.5	-10.5	22.7
10	22 040	21 365	22 878	1.7	-10.3	9.5	12.8	-1.1	21.2
50	22 000	21 348	22 644	1.7	-6.4	9.2	12.6	1.4	19.3

transpiration. Simulated runoff was much higher than measured runoff in the Deschutes River Basin, however, runoff is primarily routed through groundwater there and precipitation is not well correlated with runoff on an annual basis (T. Laenen, USGS, Portland, OR, pers. commun.).

Measured and simulated aboveground net primary productivity (ANPP) were compared at three of the OTTER sites within the modeled domain. LAI had been reduced significantly below its potential by insect damage or thinning on the other two relevant OTTER sites. Simulated ANPP was within 15% of the observed value at the two conifer-dominated sites. Simulated ANPP was 200% of the observed value at the easternmost site in the Juniper woodland, however, the measurements covered only tree productivity whereas shrubs contributed a significant proportion to total LAI. At the regional scale, these site-specific inconsistencies are less apparent. Average stem production (estimated as 1/3 of NPP) for all forested grid cells was 3120 kg/ha (expressed as carbon) compared to an estimate of 3000 to 6000 kg/ha for medium-productivity Douglas-fir (*Pseu-*

dotsuga menziesii) stands in the Pacific Northwest (Mills, 1988; Peterson and Heath, 1991).

3.2. Ten- and 50-km simulations

Although mean elevation was similar across resolutions, the characteristics of the resampled DEMs were significantly different with regard to elevation, slope, and aspect. Maximum elevation observed over the 1-km grid was 3084 m, but only 2328 m over the 10-km grid and 1822 m over the 50-km grid. The representation of the underlying drainage structure was also lost at 50-km. The maximum slope dropped from 30° at 1-km to 3° at 10-km and 1° at 50-km.

Since the interpolated climatic variables depend strongly on the DEM, their means and ranges were similarly impacted (Table 1). The mean clear sky radiation over the study area on a given day did not differ greatly at the three spatial resolutions because low values on north-facing slopes generally compensated for high values on corresponding south-facing slopes. The maximum clear sky radiation differed by at most 10% on any given day between the 1- and 50-km simulations, however, the minimums at the

Table 2
Comparison of land surface characteristics across spatial resolutions

Resolution (km)	Land cover type (%)			LAI (m ² /m ²)			WHC (cm)		
	grass	shrub	forest	Mean	Min	Max	Mean	Min	Max
1	17	21	62	4.3	1	8	16.3	10	23
10	14	21	65	4.5	1	8	16.3	10	23
50	3	22	75	4.9	1	8	16.2	10	23

1-km resolution was only 1/3 that of the 50-km resolution. These effects were associated primarily with the steeper north- and south-facing slopes at the 1-km resolution. The ranges of minimum temperature and maximum precipitation responded strongly to the contraction of the elevation range at the 1-km

resolution but, as with radiation, the means were similar across resolutions. A significant potential for sampling error with regard to precipitation was evident at the 50-km resolution since shifting the 50-km grid 10 or 20 km in all directions indicated a 20% coefficient of variation in mean annual precipitation.

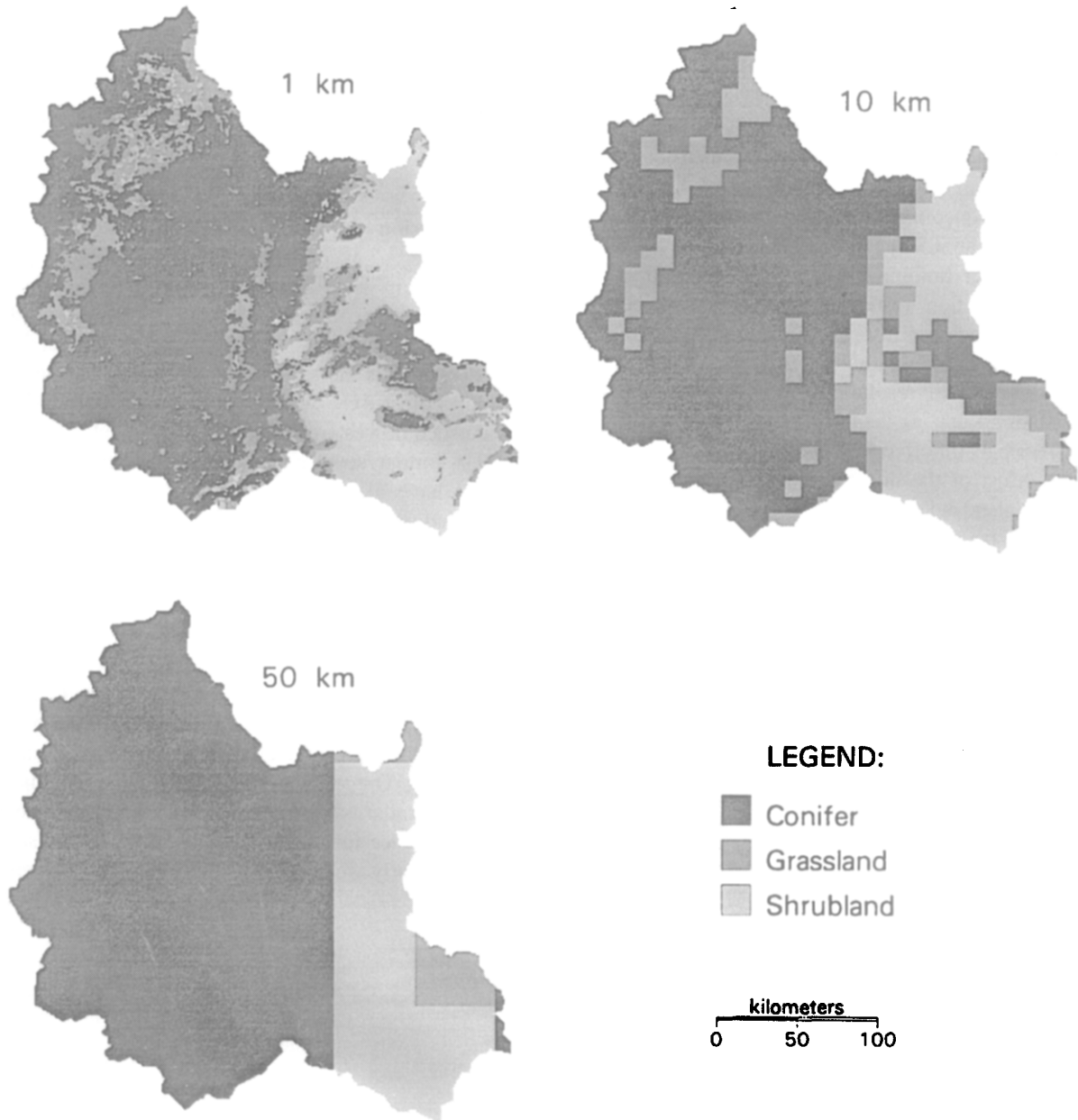


Fig. 3. Biome classification at the three spatial resolutions.

Table 3

Comparison of annual water balance variables (mm) across spatial resolutions. Mean outputs do not equal mean precipitation because of changes in storage

Resolution (km)	Precipitation			Evaporation			Transpiration			Runoff		
	Mean	Min	Max	Mean	Min	Max	Mean	Min	Max	Mean	Min	Max
1	985	97	5468	179	0	481	279	2	554	556	0	2840
10	980	100	5499	186	15	422	293	96	595	544	0	2764
50	973	178	2349	202	24	371	286	128	435	536	0	1588

The aggregation of the land surface characteristics to the coarser resolutions introduced significant changes in some cases. Forest cover increased from 61% at 1 km to 75% at 50 km (Table 2, Fig. 3). Average LAI correspondingly increased from 4.3 at 1 km to 4.9 at 50 km (Table 2). In contrast, the range in soil water holding capacity was retained at the 50-km resolution, reflecting the much lower heterogeneity in the base map for this variable.

The mean model outputs were more similar across the three spatial resolutions for the water balance variables (Table 3) than for the carbon flux (Table 4). Average runoff differed only 4% across resolutions. Most of the difference was associated with a 13% higher evaporation at the coarser resolution (Table 2) because of the higher average LAI. The net primary productivity (NPP) surfaces at 50 km were only weakly indicative of the underlying vegetation and climatic gradients and average simulated NPP over the study area at 50 km was 11% higher than at 1 km. Maintenance respiration also increased with coarsening of the spatial resolution, most likely because of the increase in stem biomass and LAI associated with more area as forest.

Although mean values for model outputs were generally similar across resolutions, difference maps (e.g., Fig. 4) indicated a large loss of spatially explicit information. The standard deviation of the

difference in NPP between the 1- and 50-km analysis was 2720 kg/ha compared to an overall mean NPP of 7560 kg/ha.

4. Discussion

The 1-km simulation came reasonably close to replicating the limited observations related to the spatial and temporal patterns in water and carbon flux over this heterogeneous region. Analyses in which Forest-BGC was distributed over a 1600-km² watershed in western Montana (Running et al., 1989) and a similar sized area in Ontario Canada (Band, 1993) have also produced general agreement with observations. Limitations in these analyses are most evident in site-specific checks which reveal discrepancies in the water balance. Poor representation of soil water holding capacity and lateral flow are significant problems. These limitations are being addressed by efforts to link a subsurface flow model to the spatially distributed Forest-BGC (Band, 1993) and to utilize the DEM and higher resolution soil maps to better characterize water holding capacity (D. Zheng, Oregon State University, pers. commun.).

The similarity between the observed and modeled water balance for the Willamette Basin in this study is particularly welcome considering earlier underesti-

Table 4

Comparison of model carbon flux variables (kg/ha) across spatial resolutions

Resolution (km)	Photosynthesis			Maintenance respiration			Potential net primary productivity		
	Mean	Min	Max	Mean	Min	Max	Mean	Min	Max
1	11344	0	25988	2315	100	6353	7563	0	17325
10	12012	3081	24034	2493	95	6016	8008	2054	16023
50	12563	3183	21325	2848	196	5568	8375	2122	14217

mation of precipitation in this region (Marks et al., 1993). In that analyses, the precipitation interpolation did not include elevation and thus tended to produce underestimates of runoff at the river basin scale (Phillips, 1992). The ability of PRISM to account for high-elevation precipitation has helped alleviate this problem.

There does not appear to be any benefit to using a resolution finer than 1 km for the purposes of simu-

lating large watershed or river basin scale runoff with the spatially distributed Forest-BGC. Band et al. (1991) initialized and ran Forest-BGC over a 17-km² watershed in western Montana using a 30-m DEM for elevations, and satellite-mounted Thematic Mapper imagery to estimate LAI. Their approach employed an algorithm which aggregates hillslopes and streams into successively larger hillslopes, and the spatially distributed model was run at each level of

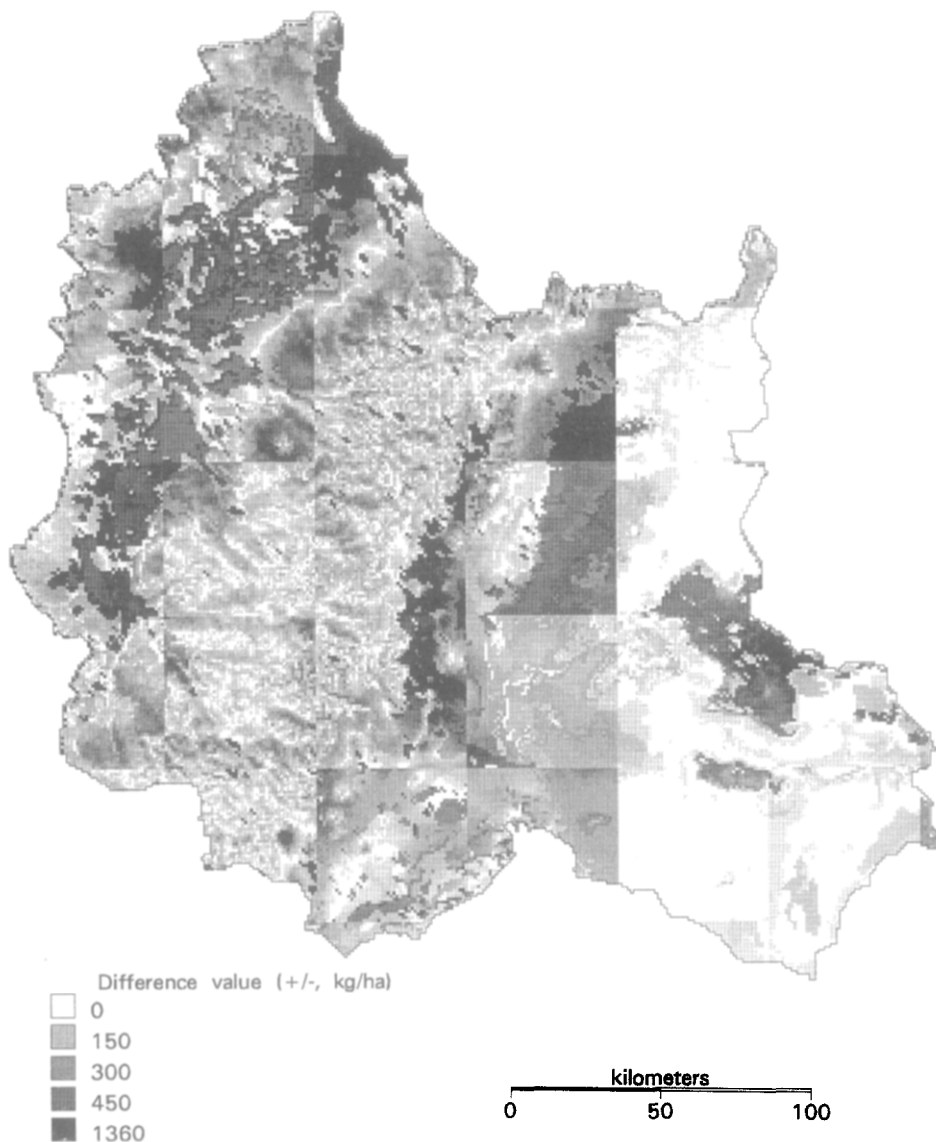


Fig. 4. Map of differences (+ or -) in net primary productivity between the 1-km resolution and the 50-km resolution.

aggregation. The simulation with six hillslopes (polygons several km on a side) gave a watershed-level average evapotranspiration and photosynthesis quite similar to the 30-hillslope simulation. Apparently, averaging values for the input variables at the coarse scale did not subsume so much variation that outputs differed significantly at the two levels of aggregation.

The study of Farajalla and Vieux (1995), which examined variability in hydrologically relevant parameters at spatial resolutions from 30–2500 m, also suggested that the spatial variation below the 1-km resolution may not be critical. Of more importance for replicating daily hydrograph data is probably inclusion of an algorithm which moderates the release and subsurface flow of soil water (Wigmosta et al., 1994). Interestingly, subsurface flow models may require DEMs at a spatial resolution somewhat finer than 1 km in some regions because of their dependence on a highly spatially resolved stream network (White and Running, 1994).

Above the 1-km resolution, the results in this study clearly indicate differences in the inputs and outputs as spatial resolution is coarsened. The trend towards a gain in the dominant land cover classes as the spatial resolution was coarsened is consistent with other scaling studies (Turner et al., 1989). In a heterogeneous forested area in Northern California, this aggregation error steadily increase from 90 m, which was considered the fundamental scale of the smaller patches of cover type, out to 5000 m (Moody and Woodcock, 1994). The spatial resolution of the MODIS sensor, the primary EOS-era instrument for mapping and monitoring the terrestrial biosphere, will range from 250 to 500 m depending on spectral band (Running et al., 1995). Thus, issues related to mixed pixels at those resolutions, and aggregation errors as resolution is coarsened to accommodate modeling needs, will become increasingly important.

The loss of information with a coarsening of the spatial resolution depends to some degree on the aggregation scheme. Averaging of fine-scale values for continuous variables is less desirable than sampling the center point of the coarse-resolution cells because averaging tends to eliminate the tails of the distributions, where impacts on processes having nonlinear response algorithms may be greatest. The hillslope-based aggregation scheme in Band et al.

(1991) is attractive because the average for temperature or radiation over a hillslope represents the mean of an even number of more north-facing or south-facing slopes. In contrast, the average for a large grid cell might represent a great variety of elevations, slope angles, and aspects. Note, however, that hillslope-based aggregation would become problematical at too coarse a resolution because the gradients in important vertically varying parameters such as precipitation would be lost.

One consequence of the increased area of forest cover at the coarse resolutions in this study was increased estimates for mean primary productivity. This effect was in part a function of the higher LAI associated with forestland compared to shrubland and grassland. The potential increase was mitigated to some extent because of: (1) lengthening of the drought stress period brought on by higher evaporation and transpiration, and (2) increased maintenance respiration associated with more stem biomass. Running the model three times within each 50-km grid cell, once for each biome type, and calculating the weighted average for the outputs, compensated for much of the difference between the 50-km and 1-km simulations; mean NPP then differed between resolutions by only 2%. The larger area of forests at the 50-km resolution also tended to reduce mean runoff but this effect was small, apparently because runoff in the Pacific Northwest is dominated by winter storms and snow melt.

The differences in model outputs which are the result of a narrower range in the climatic variables at the coarser resolutions should depend in part on the nature of the response functions in the model being used. The response functions which link radiation and temperature to the processes of evaporation, transpiration and photosynthesis in Forest-BGC are generally not linear (Running and Coughlan, 1988). Photosynthesis has a concave temperature response function with a mid-range optimum around 20°C, and respiration has an exponential response to increasing temperature. However, the contraction of the temperature range at the 50-km resolution was primarily at the cold end of the range where the metabolic rates are quite low anyway. Thus, the contribution of this factor to the differences in the mean outputs was small.

With precipitation, the reduction of the elevation

range at the coarsest resolution more than halved the maximum precipitation estimate. The effect on mean runoff, however, amounted to only a 4% difference. The small difference was, in part, because of the small proportion (2%) of the area in the 1-km DEM which was above the maximum elevation in the 50-km DEM. The actual scale of orographic precipitation, i.e. the distance over which differences in precipitation as a function of elevation or aspect have been observed, is certainly much less than 50-km (Daly et al., 1994).

Conclusions about the sensitivity of model outputs to the spatial resolution of the inputs are specific to the spatial domain, the terrain structure, and the particular model in the study. In a region such as the Great Plains of the United States, with relatively shallow environmental gradients and a more homogeneous plant physiognomy, the 50-km simulation may have yielded results more similar to the 1-km simulation than was the case here. If the spatial resolution of the analysis was expanded beyond 50-km towards that of a general circulation model (GCM) grid cell, the opportunity for sampling error would obviously increase. The ranges for model outputs (Tables 3 and 4) give some indication of the possible representative value if an arbitrary point were used for the whole 54 976 km² area (about 1/2 a 300 × 300-km GCM grid cell).

The significant loss of information at the 50-km resolution compared to the 1-km resolution may be particularly relevant to analysis of the potential effects of climatic change. Vegetation characteristics along environmental gradients have been suggested to represent analogues for changes which might be expected under altered climate regimes (Callaway et al., 1994). In areas of complex topography, the environmental gradients tend to be lost at the 50-km resolution and the finer resolution thus offers greater opportunity to explore spatial patterns in ecosystem structure and function which might aid in simulating responses to climate change.

Acknowledgements

We thank S. Running for sharing Forest-BGC, C. Daly for assistance with PRISM, and D. Jacobsen, J. Kern and J. Kimball for help in assembling the

required databases. Data sets for validating the climate interpolations were provided by the Forest Science Data Bank, a partnership between the Department of Forest Science, Oregon State University, and the U.S. Forest Service Pacific Northwest Research Station, Corvallis, Oregon. Funding for these data was provided by the Long-Term Ecological Research program and other National Science Foundation programs, Oregon State University, and the U.S. Forest Service Pacific Northwest Research Station.

References

- Band, L.E., 1993. A pilot landscape ecological model for forests in central Ontario. Report No. 7, Ontario Forest Research Institute, Ontario Ministry of Natural Resources, Toronto, Ont., Canada.
- Band, L.E., Peterson, D.L., Running, S.W., Coughlan, J., Lammers, R., Dungan, J. and Nemani, R., 1991. Forest ecosystem processes at the watershed scale: basis for distributed simulation. *Ecol. Model.*, 56: 171–196.
- Bristow, K.L. and Campbell, G.S., 1984. On the relationship between incoming solar radiation and daily maximum and minimum temperature. *Agric. For. Meteorol.*, 31: 159–166.
- Callaway, R.M., DeLucia, E.H. and Schlesinger, W.H., 1994. Biomass allocation of montane and desert ponderosa pine: An analog for response to climate change. *Ecology*, 75: 1474–1481.
- Daly, C., Neilson, R.P. and Phillips, D.L., 1994. A statistical-topographic model for mapping climatological precipitation over mountainous terrain. *Appl. Meteorol.*, 33: 140–158.
- Defense Mapping Agency, 1981. Product specifications for digital terrain elevation data, 2nd ed. D.M.A. Aerospace Center, St. Louis Air Force Station, St. Louis, MO, 23 pp.
- Dolph, J., Marks, D.G. and King, G.A., 1992. Sensitivity of the regional water balance in the Columbia River Basin to climate variability: Application of a spatially distributed water balance model. In: R.J. Naiman and J.R. Sedell (Editors), *Watershed Management: Balancing Long Term Sustainability and Environmental Change*. Springer-Verlag, New York, pp. 233–266.
- Dubayah, R., Dozier, J. and Davis, F., 1990. Topographic distribution of clear-sky radiation over the Konza Prairie, Kansas. *Water Resour. Res.*, 26: 679–691.
- Earth Info, 1988. *Climate Data Users Manual*, Denver, CO.
- Farajalla, N.S. and Vieux, B.E., 1995. Capturing the essential spatial variability in distributed hydrological modelling: Infiltration parameters. *Hydrol. Processes*, 9: 55–68.
- Franklin, J.F. and Dyrness, C.T., 1990. *Natural vegetation of Oregon and Washington*. Oregon State University Press, Corvallis, OR.
- Frew, J.E., 1990. The image processing workbench. Ph.D. Thesis, Department of Geography, University of California, Santa Barbara, CA, 382 pp.

- Glassy, J.M. and Running, S.W., 1994. Validating diurnal climatology logic of the MT-CLIM model across a climatic gradient in Oregon. *Ecol. Appl.*, 4: 248–257.
- Grier, C.C. and Running, S.W. (Editors), 1977. Leaf Area of Mature Northwestern Coniferous Forests: Relation to Site Water Balance. *Ecology*, 58: 893–899.
- Hubbard, L.E., Kroll, C.G., Herrett, T.A., Kraus, R.L. and Rupert, G.P., 1991. Water resources data: Oregon water year 1990, Volume 1. Water-Data Report OR-90-1, U.S. Geological Survey, Portland, OR.
- Hunt, E.R., Jr., Martin, F.C. and Running, S.W., 1991. Simulating the effects of climatic variation on stem carbon accumulation of a ponderosa pine stand: Comparison with annual growth increment data. *Tree Physiol.*, 9: 161–171.
- Kern, J.S., 1995. Geographic patterns of soil water holding capacity in the contiguous United States. *J. Soil Sci. Soc. Am.* (in press).
- Kimball, J., 1992. A daily climatology of the Pacific Northwest. Abstract H21-A04, Transactions of the American Geophysical Union.
- King, G.A., 1993. Net primary productivity of non-forested lands. In: D.P. Turner, J.J. Lee, G.J. Koerper and J.R. Barker (Editors), *The Forest Sector Carbon Budget of the United States: Carbon Pools and Flux Under Alternative Policy Options*. U.S. Environmental Protection Agency Environmental Research Laboratory, Corvallis, OR, EPA/600/3-93/093, pp. 179–194.
- Loveland, T.R., Merchant, J.W., Ohlen, D.O. and Brown, J.F., 1991. Development of a land-cover characteristics database for the conterminous United States. *Photogramm. Eng. Remote Sens.*, 57: 1453–1463.
- Marks, D.G., Dubayah, R. and Longley, K., 1991. Modeling the topographic and spectral variability of clear-sky solar radiation at regional to continental scales. In: Vol. 3, Proceedings of 1991 IGARSS Symposium, Remote Sensing: Global Monitoring for Earth Management, Espoo, Finland, p. 1711.
- Marks, D.G., King, G.A. and Dolph, J., 1993. Implications of climate change for the water balance of the Columbia River Basin, U.S.A. *Clim. Res.*, 2: 203–213.
- Marshall, J.D. and Waring, R.H., 1986. Comparison of methods of estimating leaf-area index in old-growth Douglas-fir. *Ecology*, 67: 975–979.
- Mills, J.R., 1988. Inventory, Growth, and Management Assumptions for the 1989 RPA Timber Assessment. Part I – The South and Part II – The North and West, Reports on file at the Pacific Northwest Research Station, Portland, OR.
- Moody, A. and Woodcock, C.E., 1994. Scale-dependent errors in the estimation of land-cover proportions: Implications for global land-cover datasets. *Photogramm. Eng. Remote Sens.*, 60: 585–594.
- Neilson, R.P., King, G.A. and Koerper, G.J., 1992. Toward a rule-based biome model. *Landscape Ecol.*, 7: 27–43.
- Nemani, R. and Running, S.W., 1989. Testing a theoretical climate–soil–leaf area hydrologic equilibrium of forests using satellite data and ecosystem simulation. *Agric. For. Meteorol.*, 44: 245–260.
- Peterson, C.E. and Heath, L.S., 1991. The influence of weather variation on regional growth of Douglas-fir stands in the U.S. Pacific Northwest. *Water Air Soil Pollut.*, 54: 295–305.
- Peterson, D.L., Spanner, M.A., Running, S.W. and Teuber, K.B., 1987. Relationship of thematic mapper simulator data to leaf area index of temperate coniferous forests. *Remote Sens. Environ.*, 22: 323–341.
- Phillips, D.L., 1992. A comparison of geostatistical procedures for spatial analysis of precipitation in mountainous terrain. *Agric. For. Meteorol.*, 58: 119–141.
- Running, S.W., 1994. Testing forest-BGC ecosystem process simulations across a climatic gradient in Oregon. *Ecol. Appl.*, 4: 238–247.
- Running, S.W. and Coughlan, J.G., 1988. A general model of forest ecosystem processes for regional application. *Ecol. Model.*, 42: 125–154.
- Running, S.W. and Gower, S.T., 1991. FOREST BGC, A general model of forest ecosystem processes for regional applications, II. Dynamic carbon allocation and nitrogen budget. *Tree Physiol.*, 9: 147–160.
- Running, S.W. and Hunt, Jr., E.R., 1993. Generalization of a forest ecosystem process model for other biomes, Biome-BGC, and an application for global-scale models. In: J.R. Ehleringer and C. Field (Editors), *Scaling Processes between Leaf and Landscape Levels*. Academic Press, San Diego, CA, pp. 151–158.
- Running, S.W. and Nemani, R.R., 1988. Relating seasonal patterns of AVHRR vegetation index to simulated photosynthesis and transpiration of forests in different climates. *Remote Sens. Environ.*, 24: 347–351.
- Running, S.W., Nemani, R.R. and Hungerford, R.D., 1987. Extrapolation of synoptic meteorological data in mountainous terrain and its use for simulating forest evapotranspiration and photosynthesis. *Can. J. For. Res.*, 17: 472–483.
- Running, S.W., Nemani, R.R., Peterson, D.L., Band, L.E., Potts, D.F., Pierce, L.L. and Spanner, M.A., 1989. Mapping regional forest evapotranspiration and photosynthesis by coupling satellite data with ecosystem simulation. *Ecology*, 70: 1090–1101.
- Running, S., Justice, C., Hall, D., Huete, A., Kaufman, Y., Muller, J., Strahler, A., Vanderbilt, V., Wan, Z., Teillet, P. and Carneggie, D., 1995. Terrestrial remote sensing science and algorithms planned for EOS/MODIS. *Remote Sensing Environ.* (in press).
- Runyon, J., Waring, R.H., Goward, S.N. and Welles, J.M., 1994. Environmental limits on above-ground production: Observations from the Oregon transect. *Ecol. Appl.*, 4: 226–237.
- Saxton, K.E., Rawls, W.J., Romberger, J.S. and Papendick, R.I., 1986. Estimating generalized soil-water characteristics from texture. *Soil Sci. Soc. Am. J.*, 50: 1031–1036.
- Soil Conservation Service, 1991. State soil geographic data base (STATSGO): data users guide. Miscellaneous Publication Number 1492, U.S. Government Printing Office, Washington, DC.
- Turner, D.P., Koerper, G.J., Gucinski, H., Peterson, C.E. and Dixon, R.K., 1993. Monitoring global change: comparison of forest cover estimates using remote sensing and inventory approaches. *Environ. Monitor. Assess.*, 26: 295–305.
- Turner, M.G., O'Neill, R.V., Garnder, R.H. and Milne, B.T.,

1989. Effects of changing spatial scale on the analysis of landscape pattern. *Landscape Ecol.*, 3: 153–162.
- USDA, Soil Conservation Service (SCS), 1988. Snow surveys and water supply forecasting. Agriculture Information Bulletin 536, Washington, DC.
- USGS, 1991. The 1990 Conterminous United States, AVHRR Data Set. U.S. Geological Survey, EROS Data Center, Sioux Falls, SD.
- Waddell, K.L., Oswald, D.D. and Powell, D.S., 1989. Forest statistics of the United States. Bulletin PNW-RB-168, USDA Forest Service Resource, Portland, OR.
- White, J.D. and Running, S.W., 1994. Testing scale dependent assumptions in regional ecosystem simulations. *J. Veg. Sci.*, 5: 687–702.
- Wigmosta, M.S., Vail, L.W. and Lettenmaier, D.P., 1994. A distributed hydrology–vegetation model for complex terrain. *Water Resour. Res.*, 30: 1665–1679.
- Woodward, F.I., 1987. *Climate and Plant Distribution*. Cambridge University Press, London.